Parallel Factor Analysis (PARAFAC) for multidimensional decomposition of fNIRS data - A validation study

Hüsser, Alejandra[*, 1,2], Caron-Desrochers, Laura[*, 1,2], Tremblay, Julie[1], Vannasing, Phetsamone[1], Martínez-Montes, Eduardo[†, 3] & Gallagher, Anne[†, 1, 2]

[*] Co-First author
[†]Co-Senior author
Corresponding author: anne.gallagher@umontreal.ca

[1] Neurodevelopmental Optical Imaging Laboratory (LIONLab)
Research Center of the Sainte-Justine University Hospital Center
3175, Chemin de la Côte-Sainte-Catherine
Montreal, QC H3T 1C5, Canada

[2] Department of Psychology
Université de Montréal
Pavillon Marie-Victorin
P.O. Box 6128 Centre-ville Station, 2900 Boulevard Édouard-Montpetit
Montreal, QC H3T 1J4, Canada

[3] Cuban Neurosciences Center (CNEURO)
Street 190 e / 25 and 27 Cubanacan
Playa Havana, CP 11600, Cuba

1 Abstract

Functional near infrared spectroscopy (fNIRS) is a neuroimaging technique that uses light at two different wavelengths in the near infrared spectrum to estimate cerebral hemodynamic response, based on concentration changes in both oxygenated and deoxygenated hemoglobin. A multi-dimensional decomposition technique, parallel factor analysis (PARAFAC), has recently been validated for the identification of artifacts and cerebral activation patterns in electroencephalography. Our objective was to introduce and validate the use of the PARAFAC model for the analysis of fNIRS data, which is inherently multidimensional (time, space, wavelength). Eighteen healthy adults underwent fNIRS acquisition during a semantic verbal fluency task. Both the signal-to-noise ratio and Pearson's correlation were used to evaluate the efficacy of PARAFAC for motion artifact correction. Temporal, spatial and hemodynamic characteristics of the PARAFAC component allowed us to validate the identification of task-related cerebral activation. Using PARAFAC, results revealed a significant improvement in data quality after movement artifact correction. Compared to traditional two-dimensional approaches (e.g. ICA, PCA), PARAFAC offered some advantages. Although PARAFAC revealed a slightly more distributed functional network, temporal and spatial characteristics of the task-related brain activation identified with PARAFAC mostly overlapped with commonly used approaches (e.g. general linear model, global average). This study describes the first implementation of PARAFAC in fNIRS and supports it as a promising data-driven alternative for multi-dimensional data analyses in fNIRS.

2 Keywords

Near-infrared spectroscopy, multidimensional decomposition, parallel factor analysis, canonical decomposition, artifact correction, language paradigm.

3 Introduction

Functional near-infrared spectroscopy (fNIRS) is a non-invasive neuroimaging technique that uses light of at least two different wavelengths in the near-infrared spectrum in order to assess brain activity based on neurovascular coupling. The specific absorption properties of oxygenated (HbO) and deoxygenated (HbR) hemoglobin allow individual assessments of concentration changes in both HbO and HbR (Jobsis, 1977). Thus, data can be interpreted not only for temporal and spatial characteristics, but also for the wavelength or hemodynamic domain. Compared to functional magnetic resonance imaging (fMRI), fNIRS offers lower spatial resolution but allows a more comprehensive representation of the hemodynamic response, and at a faster time resolution (≈ 0.1s). Currently, many of the fNIRS data analysis approaches (e.g. wavelet filtering, decomposition, spline interpolation, etc.) do not take fully into account the multidimensional structure of the fNIRS signal and are limited to two dimensions, often considering either time and space, or time and wavelength (Brigadoi et al., 2014; Cooper et al., 2012; Sungho Tak & Ye, 2014). Two-dimensional (2D) analyses require that data with more dimensions, such as fNIRS data, undergo superficial unfolding before processing, for example, treating both wavelengths or HbO and HbR independently. Hence, some of these 2D analysis tools are forced to impose other non-physiological constraints, such as orthogonality or statistical independence. To overcome these limitations, a multidimensional (≥3D) approach called parallel factor analysis (PARAFAC; Bro, 1998; Harshman, 1970), or less frequently referred to as canonical decomposition (Carroll & Chang, 1970), could be considered as an alternative for the analysis of fNIRS data.

Multidimensional decomposition was initially introduced in the field of psychometrics and linguistics as a tool for multi-factor analysis (Carroll & Chang, 1970; Harshman, 1970; Tucker, 1966). Over time, its use was extended to neuroimaging signals, such as the analysis of event-related potentials (ERPs) assessed by electroencephalogram (EEG). For this application, decomposition took into account three dimensions: time, space and participants (Field & Graupe, 1991; Möcks, 1988). Later, PARAFAC was introduced for data analysis in continuous EEG recordings, taking into account the 3D structure of the EEG signal (time × space × frequency) (Martínez-Montes, Valdés-Sosa, Miwakeichi, Goldman, & Cohen, 2004; Miwakeichi et al., 2004). The growing popularity of PARAFAC in neuroimaging stems from the intrinsic advantage of multidimensional decomposition, because most data gathered in neuroscience are naturally multidimensional. Also, the data-driven approach could enlighten new aspects of neuroimaging data (Calhoun, 2018).

PARAFAC is a decomposition technique applicable to any dataset that can be described in more than two dimensions (e.g. time, space, frequency, participants, conditions, signal characteristics) and allows for the extraction of different signatures present in the data. It assumes multilinear relations between the different dimensions and usually does not need any other mathematical constraints to find a unique decomposition of the data. It may therefore be used in the data pre-processing steps to isolate artifacts, as well as in the actual data analyses to extract a predominant brain activation, or other relevant characteristics of the signal. Indeed, using a 3D wavelet transformation in EEG data, Miwakeichi and colleagues (2004) revealed PARAFAC as an

appropriate tool for both the detection of ocular movement artifacts and the identification of dominant brain activation patterns. In this study, some of the components identified using PARAFAC were highly similar to those extracted with principal component analysis (PCA), an established approach for 2D decomposition. Specifically, significant overlap was shown for eigenvalues and peaks of time/frequency components, as well as their topographical representations found with PCA and PARAFAC. PARAFAC, using the dimensions of time, space and frequency, has also been applied successfully to the EEG data of individuals with epilepsy, for the purposes of artifact detection and the identification of aberrant cerebral activation (Acar, Aykut-Bingol, Bingol, Bro, & Yener, 2007). Overall, these studies suggest that in the context of time × space × frequency analysis of EEG data, PARAFAC achieves comparable results to well-established approaches while allowing for easier interpretation, and doing so without imposing non-physiological constraints (Martínez-Montes et al., 2004). Multidimensional decomposition with PARAFAC is not limited to 3D and could potentially be expanded to n-dimensions. In the context of ERP data, PARAFAC as a five-way analysis has successfully been used to identify differences and common characteristics of inter-trial phase coherence across conditions and subjects, including the dimensions of time, channels, frequency, subjects, and conditions (Mørup, Hansen, Herrmann, Parnas, & Arnfred, 2006).

Although PARAFAC has been applied on NIRS data in the food industry (Bro, 1998), it has not yet been used in neuroscience. Its application to fNIRS brain data could allow simultaneous analysis of temporal, spatial and wavelength dimensions, the latter codifying the information for concentration changes in HbO and HbR. Hence, after the optical intensities from both wavelengths are transformed into HbO and HbR concentration changes, it can be referred to as the hemodynamic dimension. Thus, data analyses with PARAFAC could take into account all relevant dimensions contributing to the fNIRS signal, without artificially separating information delivered by the use of multiple wavelengths in each channel. As described above, because PARAFAC does not impose independence and orthogonality constraints (e.g. Miwakeichi et al., 2004), it can therefore represent the real underlying physiological signals that are mixed in a multilinear structure.

A highly useful application of PARAFAC is that of artifact correction. Although the fNIRS signal is considered to be relatively tolerant to movement (Lloyd-Fox, Blasi, & Elwell, 2010), it does include some movement artifacts that can lead to abrupt changes in the light intensity, thus reducing the quality of data. It has been shown that the dynamics of both wavelengths provide important information for artifact detection and correction (Cui, Bray, & Reiss, 2010). However, current techniques for movement artifact correction typically consider only two dimensions of the signal's structure simultaneously (e.g. time and space) simultaneously and can only separate artifacts that are orthogonal or independent of physiologically relevant signals (Brigadoi et al., 2014; Cooper et al., 2012; Sungho Tak & Ye, 2014).

The bi-dimensional (time-space) decomposition of fNIRS data into components for the purposes of artifact correction is typically performed using principal component analysis (PCA) and independent component analysis (ICA). Although there are several ways to approach PCA (classification: James, Witten, Hastie, & Tibshirani, 2013; e.g. dimensionality reduction: Han Zhang et al., 2011), from the signal decomposition view, PCA aims to extract the principal component, that is the component that explains the greatest amount of variance of the signal (X. Zhang, Noah, Dravida, & Hirsch, 2017). It has been used for artifact removal because it helps to isolate the artifact's signature, or to extract other relevant activities in fNIRS (Cooper et al., 2012; Peng et al., 2014; Sungho Tak & Ye, 2014; X. Zhang et al., 2017). The data is decomposed into a

sum of components, each one formed by the product of two vectors: one representing the temporal principal component and the other, the corresponding topography (scores for each channel). A basic problem with PCA is that the components defined by only two signatures (time and space) are not uniquely determined. Therefore, in PCA, orthogonality is imposed between the corresponding temporal signatures of the different components (Becker, Comon, Albera, Haardt, & Merlet, 2011; Miwakeichi et al., 2004; Sungho Tak & Ye, 2014). Orthogonality is, however, a rather non-physiological constraint. Even with this restriction, the extracted principal components are not totally unique, given that the arbitrary rotation of axes does not change the explained variance of the data. This has led researchers to use different mathematical criteria as the basis for choosing specific rotations (e.g. Varimax, Quartimax, Promax). In fNIRS, PCA has also been applied to target time intervals (tPCA), that is to say only during periods where artifacts related to articulation or other head movements occurred, instead of during the entire unsegmented signal (Behrendt, Firk, Nelson, & Perdue, 2018; Yücel, Selb, Cooper, & Boas, 2014). This type of targeted correction resulted in better signal quality, as compared to two other approaches, while also reducing the risk of altering the signal's global integrity (Yücel et al., 2014). We therefore decided to use the tPCA approach for our analyses in this study.

More recently, ICA has become a popular tool for this type of decomposition in fNIRS (e.g. Kamran, Mannan, & Jeong, 2016; Tachtsidis & Scholkmann, 2016; H Zhang et al., 2010). It has the benefit of preventing rotational freedom (Jung, Theis, Puntonet, & Lang, 2001). However, uniqueness is achieved at the cost of necessitating the imposition of a constraint even stronger than orthogonality, namely, statistical independence of the temporal signatures (Comon, 1994; Jutten & Herault, 1991). Statistical independence is appropriate for identifying reproducible artifact signatures (e.g. ocular movements). In ICA, the maximal number of components (hypothesized sources) equals the number of observations, which in neuroimaging is often rather high. Therefore, if too high a number of components is selected, it could become difficult to identify the artifact's signature, which could be split into several components.

In addition to being used for movement artifact correction, PARAFAC could also be considered as a tool for the analysis of the hemodynamic response. Typically, cerebral activation is characterized by a relative increase of the HbO concentration level, with a slight decrease of the HbR concentration level (Boas et al., 2001; Obrig, Rossi, Telkemeyer, & Wartenburger, 2010; Quaresima, Bisconti, & Ferrari, 2012; Schroeter, Kupka, Mildner, Uludağ, & von Cramon, 2006). Despite the advantage of measuring signals that reflect both HbO and HbR concentration changes, the estimation of cerebral activation in fNIRS studies is often mainly based on HbO concentration changes (Quaresima et al., 2012; Wolf & Greisen, 2009). This is because the HbO increase is often easier to identify than changes to HbR concentration, due to its greater amplitude and the higher signal-to-noise ratio. Furthermore, contradictory findings exist regarding the occurrence of HbR decrease, which is also why many studies favor the interpretation of HbO concentration changes only, without further investigation of HbR changes. However, ignoring concentration changes in HbR poses the risk of false positive results, because higher levels of HbO could actually, for example, be due to an artifact (Cui et al., 2010). Simultaneous treatment of both wavelengths or HbO and HbR with PARAFAC would help to overcome this limitation and allow for the identification of typical hemodynamic signatures, i.e. increase of HbO and slight decrease of HbR.

Therefore, the main objective of the current study is to validate PARAFAC for the decomposition of the fNIRS signal to 1) extract and correct movement artifacts, and 2) characterize task-related brain activation. For that purpose, we acquired fNIRS data of 18 healthy adults while they performed aloud a semantic verbal fluency task. First, we compared the use of PARAFAC to

two commonly used decomposition techniques for motion artifacts (target PCA (tPCA), and independent component analysis or ICA). Subsequently, we evaluated the spatial and temporal characteristics of language-related brain activation as identified with the PARAFAC model, and compared them to those revealed by commonly used approaches (general linear model (GLM), global average).

4 Methods

4.1 Sample

Eighteen native French-speaking adults (M_{age} = 22.8 years, SD = 2.0 years; female = 10 / male = 8) participated in this study. Inclusion criteria were: being French unilingual (no second language acquired before the age of five), right-handed, born at term, having normal hearing, normal or corrected-to-normal vision, and no history of neurological, chronic or psychiatric disorders. Experimental procedures were approved by the local ethics committee.

4.2 Procedure and verbal fluency task

Participants sat comfortably in a soundproof and electrically shielded room. They were instructed to relax, to avoid any intentional movements or muscular tension, and to fix their gaze on the center of a screen placed at a distance of 114 cm. After the installation of a cap which held optodes and detectors, participants underwent a fNIRS recording while they performed a verbal fluency task previously validated for expressive language-related activation (Gaillard et al., 2003; Gallagher, Tremblay, & Vannasing, 2016; Paquette et al., 2015). The task consisted of 11 different semantic categories (e.g. animals, colors, fruits, etc.), for which participants had to say aloud as many words as possible for each category. The name of the category was presented visually on the screen (Presentations®, Neurobehavioral Systems, 2018). We used a block design paradigm in which periods of rest (fixation cross presented on the screen) and task (semantic category) alter in 30-seconds intervals. A video camera filmed the entire session, allowing for the visual identification of movements during offline pre-processing. Audio data was used to count the number of words reported per category and to identify the timing of the words, since articulation can induce movement artifacts.

4.3 fNIRS data acquisition

fNIRS data was acquired using a frequency-domain fNIRS device (Imagent Tissue Oxymeter, ISS Inc., IL, USA) equipped with 60 emitters, each regrouping two light sources of different wavelengths (690 and 830 nm), and 14 detectors. Emitters and detectors coupled at a distance of 3-4.5 cm allowed for the recording of a total of 106 channels for both wavelengths. Optodes were held in place perpendicularly, using a cap that was fitted on the head of participants in accordance with the 10-20 system(Klem, Lüders, Jasper, & Elger, 1999). Optical intensity was measured with a sampling rate of 19.53 Hz (Boxy, ISS Inc., IL, USA). The setup covered both hemispheres equally and included the regions of interest for the investigation of language functions, i.e. frontal, temporal and parietal lobes (see Figure 1). Two short-distance emitter-detector pairs with a distance of one cm were placed at the midline in the occipital region and on the participants' wrist. These short-distance pairs enable the control for continuous physiological

contamination (cardiac frequency, respiration, Mayer waves) in the superficial layer, which is not directly related to cerebral activation (Brigadoi & Cooper, 2015; Scarpa et al., 2013).

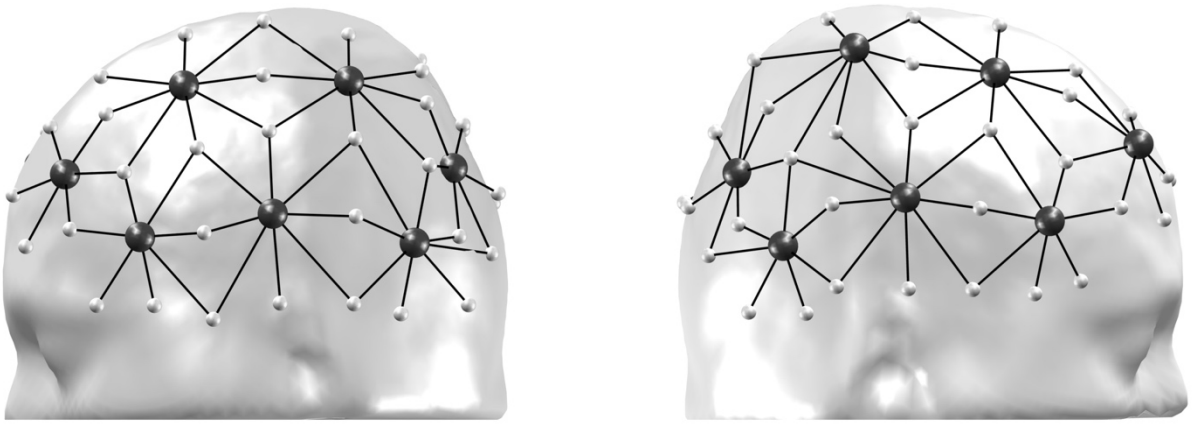

Figure 1. fNIRS setup with 14 detectors (large dark circles), and 60 light emitters (small light dots) each sending light at two different wavelengths (λ= 690 and 830 nm). The reflection of light emitted by each source is captured by one or several proximal detectors. The combination of a light emitter and a detector represents a channel (dark grey lines), for a total of 106 channels.

4.4 Pre-processing

Data analysis was conducted with the use of a homemade toolbox (LIONNIRS created by J. Tremblay, eng.) adapted in SPM12 (Statistical Parametric Mapping; Villringer & Dirnagl, 1995) in MATLAB® (The MathWorks, Inc., MA, USA). Pre-processing steps included segmentation of the signal into blocks of 50 seconds (5s resting-state baseline, 30s task and 15s resting-state). Every block was normalized by dividing each time point by the mean of the baseline. A low-pass filter with a cut-off frequency of 0.2 Hz was applied, in order to remove oscillations caused by heartbeat and respiration.

4.5 Movement artifact detection and correction

Since our language paradigm required participants to name words aloud, artifacts were mostly due to facial movements related to the muscular contraction of articulation. We performed a semi-automatic artifact detection using primarily an algorithm, to mark segments where an abrupt change exceeded three times the average variance of the signal (e.g. Aarabi & Huppert, 2016). Visual inter-rater inspection based on the signal's characteristics combined with the video recording led to the final identification of the time intervals with artifacts. These time intervals would subsequently be used to compare the efficacy of different movement artifact correction techniques intended to increase the signal quality (see section 4.7 on statistical analysis). Artifact correction was then applied to these segments using PARAFAC and two commonly used 2D decomposition techniques in fNIRS, namely those of tPCA and ICA.

4.5.1 Two-dimensional signal decomposition for artifact detection and correction

For both ICA and tPCA, the decomposition of the 2D data matrix X (whose elements x_{ij} are indexed by i channel and j time points), leads to N_f components as defined in equation 1 and illustrated in Figure 2. The matrix X_{ij} combines two separate data matrices (X_{1ij}, X_{2ij}) in order to take into account the 2D structure for both wavelengths. The maximum number of components N_f could be equal to or less than the X matrix dimension, i.e. number of channels or number of time points. Each component is modeled as the product of two factors/vectors ($a_{if} b_{jf}$) which represent signatures of the space a_{if} and time dimensions b_{jf}. The unexplained part of the data is considered irrelevant activity or noise (ε_{ij}).

(1) $x_{ij} = \sum_{f=1}^{Nf} a_{if} b_{jf} + \varepsilon_{ij}$

tPCA was integrated into our homemade LIONnirs toolbox. Artifact correction with tPCA was performed on each time interval previously identified as containing artifacts. From the obtained components we subtracted only the first, which explains most of the variance. This is in keeping with the assumption that the highest variance in the data for each segment is caused by the artifact.

Artifact correction with ICA was done using Brain Vision Analyzer (Brain Products GmbH, Gilching), and followed the steps proposed by Plank (2013). First, raw fNIRS data were exported and ICA was applied on the entire unsegmented signal, as per the method commonly reported in the literature (H Zhang et al., 2010). Noisy intervals reflecting artifacts were identified by semi-automatic inter-rater artifact detection, as explained in section 4.5. We selected components based first on their time course, i.e. high variation of light intensity similar to the artifact signature. Secondly, we rejected those whose subtraction would induce artificial artifacts elsewhere. Data was subsequently imported back into SPM. Then, segmentation and normalization were applied, as described in section 4.4.

4.5.2 Multidimensional signal decomposition

The fNIRS data naturally offers the time courses of all channels for two wavelengths, i.e. two separate data matrices. This data can be arranged in a tri-dimensional array, as illustrated in Figure 2a. In this study, we used this 3D array of the parallel factor model (PARAFAC), a multidimensional decomposition technique, for 1) performing artifact correction, and 2) studying the brain response during a language task.

The 3D array will be used for the artifact correction application. The dimensions are time (indexed by the time points in the analyzed segment), space (indexed by 106 channels) and wavelength (indexed by the two wavelengths). As explained above, PARAFAC establishes a trilinear decomposition of each element of the fNIRS data array (X_{tmw}) in N_f components, each being the product of three factors (Bro, 1998):

(2) $X_{tmw} = \sum_{f=1}^{Nf} a_{tf}\, b_{mf}\, c_{wf} + \varepsilon_{tmw}$

The estimated factors, a_{tf}, b_{mf} and c_{wf} are the elements of the so-called loading matrices $A, B\ and\ C$, whose column vectors $a_f = \{a_{tf}\}$, $b_f = \{b_{mf}\}$, $c_f = \{c_{wf}\}$, will represent the

temporal, spatial and wavelength signatures of each component (Figure 2). The uniqueness of the solution is guaranteed when the number of components (N_f) is smaller than the sum of the ranks of the three loading matrices. In the case of noisy data, it is very likely that the loading matrices are always full rank, so uniqueness is guaranteed as long as the number of components (N_f) is smaller than half the sum of the number of time points (N_t), number of channels (N_c), and number of wavelengths (N_w): $Nf \leq \frac{(N_t+N_c+N_w)}{2} - 1)$. For instance, even in a small array of 20 time points and eight channels at two different wavelengths, a unique decomposition could be achieved, using up to 14 components ($20(t) + 8(m) + 2(w) = 30 \div 2 = 15 - 1 = 14(Nf)$). Computationally, the decomposition is achieved by the Alternating Least Squares algorithm, as it has been used in previous studies on neuroscience data (e.g. Acar et al., 2007; Martínez-Montes et al., 2004; Miwakeichi et al., 2004; Mørup et al., 2006).

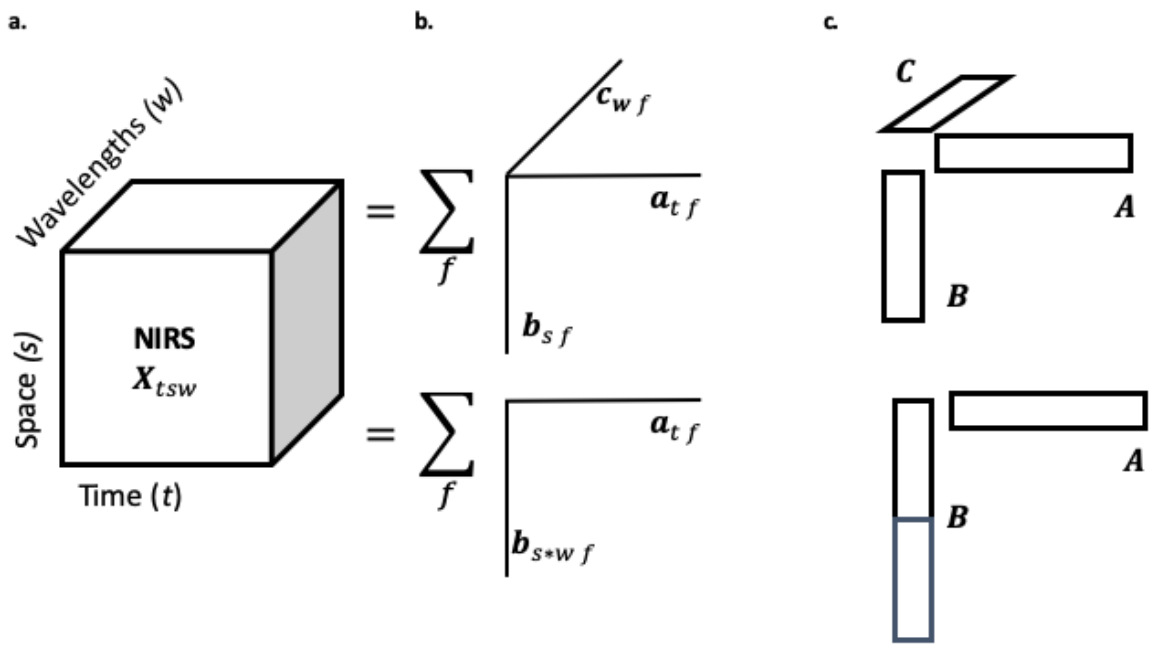

Figure 2. Schematic representation of the decomposition models applied to fNIRS data. (a) The data X is arranged as a 3D data array with its dimensions being those of time (t), space (s) and wavelengths (w). (b) PARAFAC decomposes this array into the sum of components, each being a trilinear product of loading vectors representing temporal ($a_{t\,f}$), spatial (channel, $b_{s\,f}$) and spectral (wavelength, (b_{s*wf})) signatures. tPCA/ICA decompose the array into components, each being a bilinear product of the loading vectors representing temporal ($a_{t\,f}$) and spatial signatures ($b_{s*w\,f}$). The wavelength signatures (cw_f) are represented in components including both wavelengths ($bs * w$), without taking into account their spatial dependence. (c) PARAFAC consists of finding the matrices $A = \{a_f\}$, $B = \{b_f\}$ and $C = \{c_f\}$ that explain X with minimal residual error. tPCA and ICA specifies the matrices $A_w = \{a_f\}$, $B_w = \{b_f\}$, where the relative contribution of the different wavelengths is implicitly included in the first and second halves of the rows of matrix B. For example, for the same temporal signature of each component, there will be two topographies corresponding to the two wavelengths.

The main advantage of this method is that it provides a unique decomposition of the fNIRS data into components that reflect different activities that do not need to be orthogonal or statistically independent in any of the dimensions. As long as there is any activation resulting from a different behavior in one of the dimensions, it can be extracted as a separate component. The only indeterminacy in the least square solution is the order of the components and the relative scaling of the signatures. The spatial dependency between wavelengths is therefore exploited in order to perform the decomposition. In this work, we included the PARAFAC implementation from the N-way Toolbox (Andersson & Bro, 2000) into our homemade toolbox (LIO_{NIRS} created by J. Tremblay, eng.) so as to visualize and apply the decomposition exclusively during selected time intervals and channels. Components are ordered according to their importance in explaining the data's variance (similar to PCA). The temporal scale used to visualize the components is kept intact, while the other dimensions are normalized so as to have Frobenius norms equal to one.

Since measures from both wavelengths are sampled simultaneously at each specific position on the scalp, movement artifacts affect their amplitudes similarly. During time intervals containing artifacts, the time courses of the signal from the two wavelengths commonly show a drastic and correlated increase as compared to the task-related or baseline signal (Cui et al., 2010). By using multidimensional PARAFAC decomposition, we can take advantage of this information for the adequate selection of components of the artifact's signature.

PARAFAC decomposition was specified to sort between two to four components, representing the artifacts characteristics and allowing a clear separation of the artifact signature from the rest of the signal. The appropriate components were selected based on (1) a visual inspection of their temporal overlap with the artifact, (2) the smallest number of possible components that would sufficiently correct the artifact, and (3) components showing similar weights for both wavelengths. Usually, one to three components were needed in order to achieve a satisfactory correction of the artifact, without removing the characteristics related to the true cerebral activity.

4.6 Characterizing fNIRS activation patterns

As a second step, to the clean signal we applied PARAFAC and other commonly used methods, to characterize activation patterns and assess the utility of PARAFAC to model the brain response in fNIRS. First, the optical intensity of the two wavelengths was transformed into relative concentration changes of HbO and HbR, done so by use of the modified Beer-Lambert Law (Kocsis, Herman, & Eke, 2006). For each participant, all blocks underwent detrending in order to align the beginning and end of the segments. Then, in order to characterize the cerebral activation pattern related to the verbal fluency task, three different approaches were applied to the 30-s task period of each block: (i) the General Linear Model (GLM), (ii) the global averaged concentration changes of each channel, and (iii) the PARAFAC analysis.

<u>(i) General linear model (GLM)</u> assumes that there exist linear relations between different inputs (Friston, Ashburner, Kiebel, Nichols, & Penny, 2011). It has been applied in several fNIRS studies to specify the hemodynamic response function (Minagawa-Kawai et al., 2011; Schroeter et al., 2004; Sungho Tak & Ye, 2014). For each participant, the task-related cerebral activation (y) is modeled separately for every single block, using a GLM defined as follows in Equation 3.

$$(3)\ y = ß_0 + ß_1 a + ß_2 b + \varepsilon$$

In this equation, $ß_0$ is a constant. $ß_1$ represents the relative contribution of the modeled hemodynamic response (Glover, 1999) (concentration changes of HbO and HbR respectively) based on the temporal characteristics of the stimuli defined in a. $ß_2$ represents the contribution of physiological components measured with the short-distance (< 1cm) source-detector pair b, and ε represents the unexplained part of the data related to noise or other unknown sources. $ß_1$of each channel was averaged across blocks and used in a one sample t-test against 0 to identify channels showing significant temporal overlap with the hemodynamic response function, which was modeled based on the stimuli presentation. This allowed to derive the temporal and spatial characterization of the dominant cerebral activation pattern during the semantic verbal fluency task, as revealed by the GLM.

(ii) The computation of the global averaged concentration changes of each channel is a straightforward approach to explore the spatial distribution of the task-related hemodynamic response (Sungho Tak & Ye, 2014; X. Zhang et al., 2017). The relative weight of the short-distance channel ($ß_2$) allows for the subtraction of physiological components from the fNIRS signal. The global average of HbO and HbR concentration changes, for every channel and across each block, is calculated on the corrected signal. For each block, the data used is from 5 to 20 seconds after task onset. Channels with significant concentration changes are identified using T-tests on each channel's average signal as compared to 0.

(iii) PARAFAC. A PARAFAC decomposition with a single component was applied for each block of each participant's data set after the subtraction of physiological noise from the short-distance channel ($ß_2$). We assumed that after removing artifacts and physiological noise, the activation related to the verbal fluency task would stand out as the main component of the PARAFAC decomposition. In some cases, we obtained an "inverted" component, i.e. that loaded negatively on channels, and indicated a decrease in concentration changes of HbO related to the task instead of an increase, with the inverse phenomenon for HbR. Thus, in order not to change the meaning of the data, in this particular case, the signatures obtained by PARAFAC were subjected to a sign adjustment. We based ourselves on the experimental fact that HbO concentration changes are typically higher than those for HbR. Then, the sign of each pair of signatures was changed to obtain components that represented activation scores of HbO higher than those of HbR, while the mean of the temporal signature remains positive (see Figure 6 in Appendix for a detailed description of the different cases found). This type of empirical adjustments has also been reported in other neuroimaging studies (Bro & De Jong, 1997; Mørup et al., 2006) (Bro & De Jong, 1997; Mørupe et al., 2005).

Similar to the coefficient in the GLM, which indicates how much the signal of a specific channel contributes to the modeled hemodynamic response based on the time course of the stimuli, the temporal signature of the PARAFAC component should represent the time course of the cerebral activation related to the task. The spatial signature shows how much each channel contributes to this component (topography), and the hemodynamic signature contains two relative scores specifying how much its activation is represented in the HbO and HbR signals.

4.7 Statistical analysis

In order to evaluate the use of PARAFAC for the correction of movement artifacts in fNIRS data, its performance is compared to the well-established 2D decomposition techniques (tPCA and ICA), with the use of two quality measures.

First, we calculated an estimation of the signal-to-noise ratio (SNR), as defined by Sweeney and colleagues (2012):

(4) $SNR = 10log_{10}\frac{\sigma_x^2}{\sigma_e^2}$

Here, σ_x^2 represents the signal's variance computed in segments of data, where no artifacts were identified, while σ_e^2 represents the variance of the analyzed signal in a segment where an artifact was identified. As the latter will usually be higher than the former (since it comprises both the variance of the physiological signal and the variance of the artifact), the SNR is expected to be negative whenever an artifact is present in the analyzed segment. After removing the artifact from the analyzed signal, the SNR is computed in order to identify how effectively the artifact was removed from the signal. A zero value for the SNR would indicate equal variances, meaning that an artifact was eliminated to the extent that the corrected signal does not differ from periods in which no artifact was identified. A negative value would suggest that there is some remaining variance from the artifact, and a positive value would suggest that elimination of the artifact probably subtracted part of the relevant physiological activity. Repeated-measures analysis of variance (ANOVA) and post-hoc tests with Bonferroni corrected p-values were used to compare statistically the differences between the SNR of the uncorrected signal and the signal corrected with the three different methods for artifact correction.

Then, Pearson's correlation coefficient between the time courses for both wavelengths was used as a measure of the efficiency of the artifact correction (Cui et al., 2010). This is in line with the assumption that a high correlation coefficient indicates the presence of artifactual signals, since in a clean signal these temporal courses appear much less correlated. We used Fisher's transformation to convert correlation coefficients into z-values to obtain an approximately normal distribution. Repeated-measures ANOVA allowed for the comparison of the mean Pearson's correlation coefficient between the uncorrected segment to those corrected, and this for each of the three methods as well as for a time interval without artifacts (5-s baseline at rest). Pearson's correlation of the 5-s baseline served as a reference for a segment without artifacts and with no task-related cerebral activation.

Regarding brain activation related to the verbal fluency task, we aimed to compare temporal (time), topographical (space), and hemodynamic (HbO/HbR) results specified by the PARAFAC component with results from the hemodynamic response function (HRF) estimated with the GLM, as well as the global average for each channel. Temporal and hemodynamic characteristics were visually compared, based on time courses of the task-related concentration changes in HbO and HbR within the regions of interest (ROI) as revealed by each of the three methods (PARAFAC, GLM, global average). Our ROI were defined as the left Broca's area, according to Brodmann 44, 45, and its homologous channels in the right hemisphere as the right Broca's area (see Figure 4). Comparisons of the spatial characteristics of the task-related activation are conducted for the mean concentration changes of every channel. A one-sample t-test between the relative weight (PARAFAC), the $ß_1$(GLM) and the mean HbO and HbR concentration changes (global average) is tested against 0.

5 Results

From the whole sample of 18 participants, one participant was excluded from analyses, as artifact detection revealed a signal containing too many segments with noise, thus precluding the use of the quality measures to compare artifact correction techniques. The final sample for the validation of using PARAFAC for artifact correction included 17 participants who, on average,

completed 10.4 ± 0.9 blocks of the verbal fluency task. During each 30s-blocks of the verbal fluency task, participants named an average of 14 ± 2.2 words.

5.1 Artifact correction

Figure 3 provides an example of target artifact correction with PARAFAC and tPCA, illustrating the difference between the 2D and 3D target decomposition for motion artifact correction. Time courses of the PARAFAC decomposition with three components allowed for easy differentiation between two components, their distinct artifact signatures, and one component representing the clean signal (Fig. 3b). We were able to identify components that showed similar characteristics for both wavelengths, based on the wavelength weights (Fig. 3d). Artifacts are known to affect both wavelengths similarly, thus equal contribution to a component of both wavelengths is considered a reliable characteristic of an artifact component (Cui et al., 2010). On the *one* hand the principal component of tPCA seems to catch the characteristics of one of the two distinct artifacts, but not both (Fig. 3e). Signal correction that uses the two PARAFAC components (Fig. 3g) subsequently results in a less noisy time interval. TPCA, on the other hand, only seems to achieve a partial correction.

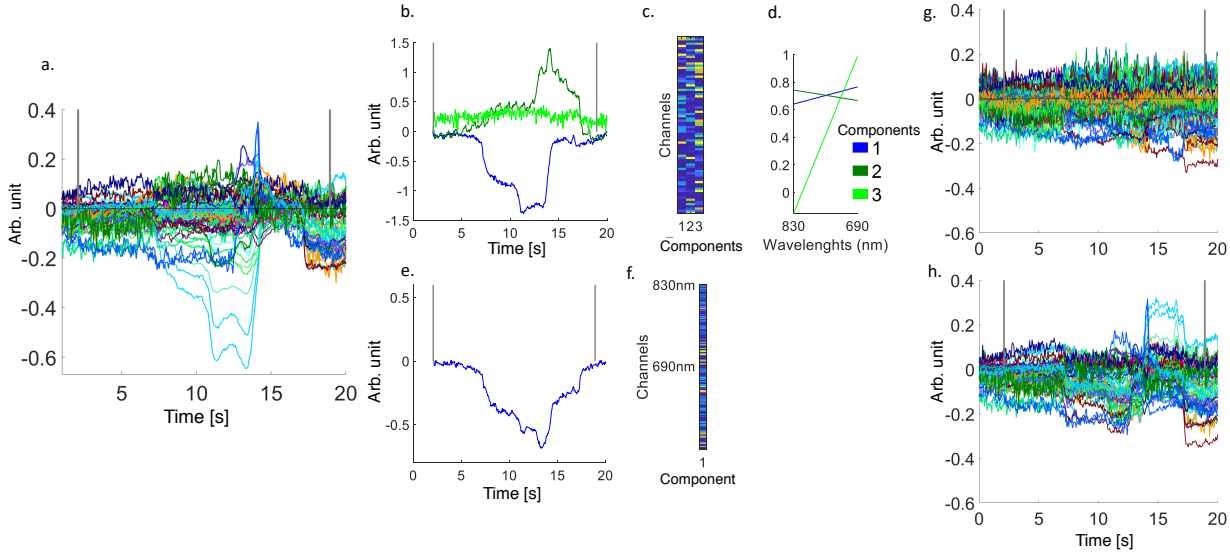

Figure 3. Example of target 3D PARAFAC and 2D tPCA decomposition to correct motion artifacts in a fNIRS data set. (a) shows the uncorrected segment. (b), (c) and (d) illustrate temporal, spatial (channel) and wavelength characteristics of the components identified with PARAFAC. (e) and (f) include the temporal and spatial characteristics of the signal, as revealed by the principal component of tPCA. (g) and (h) reveal the corrected signal, illustrating the efficacy of movement artifact correction with PARAFAC and tPCA respectively.

Our comparison of the signal-to-noise ratio (SNR) included 1,401 time intervals with previously identified artifacts, and which contained a total number of 19,630 channels for HbO/HbR. The uncorrected signal with artifacts has a SNR value of M = -0.69 dB (SD = 0.65 dB); the signal corrected with PARAFAC, M = -0.31 dB (SD = 0.58 dB); tPCA, M = -0.33 dB (SD =

0.58 dB); and ICA, M = -0.50 dB (SD = 0.64 dB) respectively. Repeated-measures ANOVA for all conditions (signal without correction, signal corrected with PARAFAC, tPCA or ICA) revealed a significant global effect, F (2.3, 44966.3) = 7550.7, $p < 0.001$, $\eta = 0.28$. Pairwise comparisons with Bonferroni correction indicate a significant difference between all SNR. All three artifact correction methods have an increase, as compared to the uncorrected signal, thus suggesting that all of them resulted in a significant improvement of the signal's quality, as compared to the uncorrected signal (see Table 1). According to the mean SNR, PARAFAC achieves the highest correction, followed by tPCA and then ICA. As the number of segments used for statistical analyses was rather large, it is relevant to consider effect sizes. The differences between the SNR of the PARAFAC corrected signal and the uncorrected signal, as well as between PARAFAC and ICA corrected signal, represent large effects ($\eta = 0.45$ and $\eta = 0.13$, respectively; Cohen, 1988). The difference in SNR between tPCA and PARAFAC corrections is a rather small effect ($\eta = 0.002$).

Table 1

Pairwise comparisons of the signal-to-noise ratio between correction techniques and the non-corrected signal

	Mean Signal-to-noise ratio in dB (SD)	PARAFAC	tPCA	ICA
Uncorrected	-0.69 ± 0.65	-0.38*	-0.37*	-0.19*
PARAFAC	-0.31 ± 0.58		0.01*	0.19*
tPCA	-0.33 ± 0.57			-0.18*
ICA	-0.50 ± 0.64			

Note. Parallel factor analysis (PARAFAC); target principal component analysis (tPCA); independent component analysis (ICA). The table contains the mean differences between the signal-to-noise ratio of the time interval with artifacts for the uncorrected signal, and the signal where the three different motion artifact correction techniques, PARAFAC, tPCA and ICA, were applied.
*Significant difference at $p < 0.001$ after Bonferroni correction for multiple comparisons.

Within segments with artifacts (n= 9815), Pearson's correlations between the time courses of the signal of both wavelengths was computed for all channels. Mean correlation coefficients across all these segments were compared for the uncorrected segment, the one corrected with each of the three different motion artifact correction techniques, as well as the artifact-free baseline

period. During the baseline, the time courses of the different wavelengths correlated on average at r = 0.47 (SD = 0.33). Both wavelengths correlated on average at r = 0.74 (SD = 0.29) for the uncorrected segments, at r = 0.51 (SD = 0.38) after PARAFAC correction, at r = 0.53 (SD = 0.38) after tPCA correction, and at r = 0.67 (SD = 0.38) after ICA correction. The highest mean correlation thus corresponded to the uncorrected signal with artifacts, followed by ICA, tPCA, PARAFAC, and finally, the baseline reference.

Mean correlation coefficients of all channels were transformed into z-scores using Fisher transformation, in order to achieve approximately normal distribution. Repeated-measures ANOVA reveals a significant difference between the five conditions: F (3.2, 30969.8) = 1908.8, p < 0.01, η = 0.16. Pairwise comparisons with Bonferroni corrected p-value for multiple comparisons further indicate significant differences of Pearson's correlation of the time course of both wavelengths between PARAFAC and all other conditions (see Table 2): 1) PARAFAC vs. uncorrected signal: $p < 0.001$, $\eta = 0.35$; 2) PARAFAC vs. tPCA: $p < 0.001$, $\eta = 0.01$; 3) PARAFAC vs. ICA: $p < 0.001$, $\eta = 0.14$; and 4) PARAFAC vs. baseline: $p < 0.001$, $\eta = 0.01$.

Differences in Pearson's correlation coefficients between the PARAFAC corrected signal and the uncorrected signal, as well as between PARAFAC and ICA corrected signal, represent large effects (η = 0.43 and η = 0.18, respectively; Cohen, 1988)). Differences in correlation coefficients between PARAFAC and tPCA, as well as between PARAFAC and the baseline signal, represent small to medium effects (both η = 0.02).

Table 2

Mean Pearson's Correlations between wavelengths

	Mean Pearson's correlation (±SD)	PARAFAC	tPCA	ICA	Baseline
Uncorrected	0.74 ± 0.29	0.228*	0.203*	0.063*	0.272*
PARAFAC	0.51 ± 0.38		0.025*	0.165*	0.044*
tPCA	0.53 ± 0.38			0.150*	0.069*
ICA	0.67 ± 0.38				0.209*
Baseline	0.47 ± 0.33				

Note. The table shows the mean differences between the Pearson's correlations of the time interval with artifacts for the uncorrected signal, the time interval for which the three motion artifact correction techniques, PARAFAC, tPCA and ICA were applied, and also for the baseline segment at rest, where no artifact was identified.

*Bonferroni corrected p-value for multiple comparisons: $p \leq 0.001$.

5.2 Characterization of task-related cerebral activation

Four participants were excluded for the characterization of brain activation, for a total of 14 participants included in the analyses. In addition to the one excluded for the first part of the study (motion artifact correction), three participants did not achieve satisfactory data quality even after artifact correction (i.e. too many channels were missing due to aberrant amplitude or frequency).

The complete topographical representation of all significant cerebral activation for the three approaches, PARAFAC, GLM, and global average, are illustrated in Figure 4. Results revealed significant activation within our ROI for all three approaches (see Table 3).

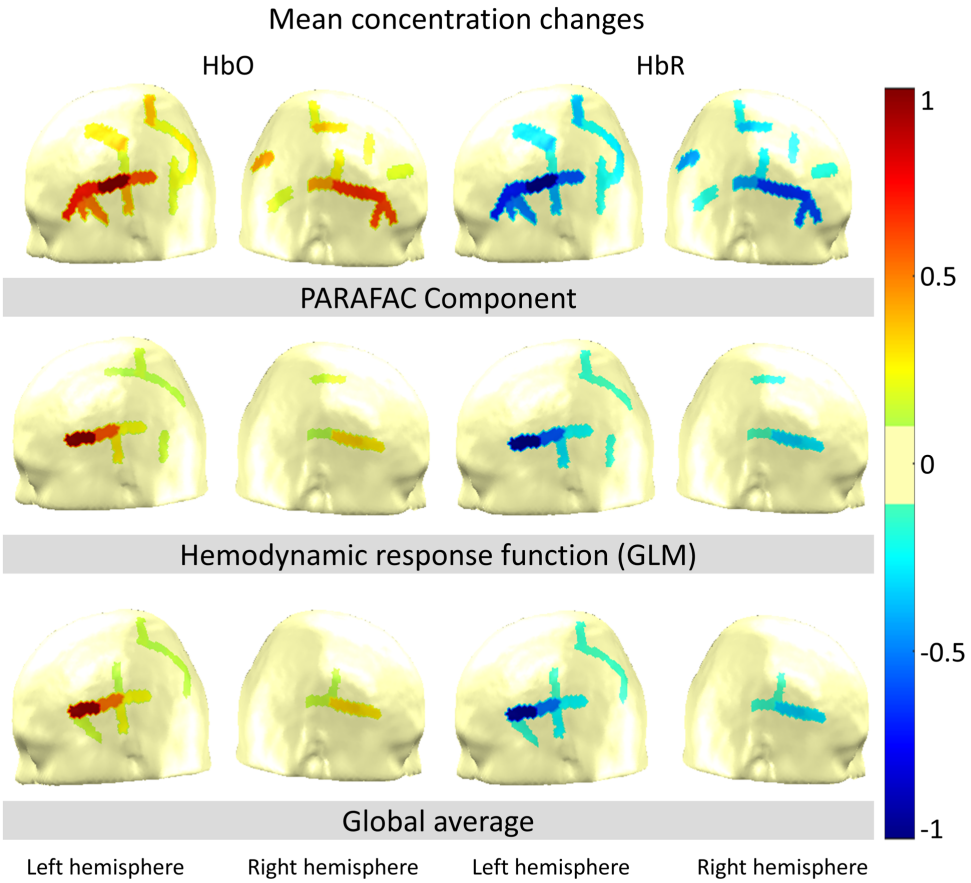

Figure 4. Topographical representation of significant task-related cerebral activation. Cerebral activation as revealed by the PARAFAC component (i.e. time dimension × hemodynamic dimension), the HRF from the GLM, and global average during 30s verbal fluency task. Only significant mean concentration changes in HbO (left) and HbR (right), as revealed by the one-sample t-tests against 0, are illustrated ($t \geq 1.64$ for HbO, $t \leq -1.64$ for HbR; one-tailed $p < .05$). Relative contribution of each method (i.e. mean relative weights for the PARAFAC component, mean Beta values for the HRF specified in the GLM, and global average per channel) are displayed in a relative scale ranging from -1 to 1. A value of 1 indicates maximum increase of HbO concentration, a value of -1 represents a maximum decrease of HbR concentration.

Table 3

Significant task-related cerebral activation associated to the verbal fluency task as revealed with PARAFAC, GLM and global average for left and right Broca's areas

	PARAFAC		GLM		Global average	
	HbO	HbR	HbO	HbR	HbO	HbR
	t-value Mean concentration changes (μM) ± standard deviation					
Broca Left	4.89*	-4.89*	5.88*	-5.88*	6.11*	-6.11*
	0.09 ± 0.22	-0.02 ± 0.04	0.04 ± 0.09	-0.01 ± 0.02	0.97 ± 1.97	-0.19 ± 0.29
Broca Right	3.91*	-3.91*	2.91*	-2.91*	3.24*	-3.24*
	0.06 ± 0.17	-0.01 ± 0.03	0.02 ± 0.06	-0.003 ± 0.01	0.39 ± 1.48	-0.08 ± 0.29

Note. Relative contribution of channels in the ROI was evaluated using mean relative weights for the PARAFAC component, mean $ß_1$ values for the HRF from the GLM, and global average for concentration changes. For each method, mean relative contribution during the 30s of the verbal fluency task was tested against 0 by use of a one-sample t-test.
*One-tail $p < 0.05$.

Figure 5 is an illustration of the temporal courses of the task-related cerebral activation obtained from the PARAFAC component, GLM and global averaging within our ROIs (left and right Broca's area) during the 30s period of the verbal fluency task.

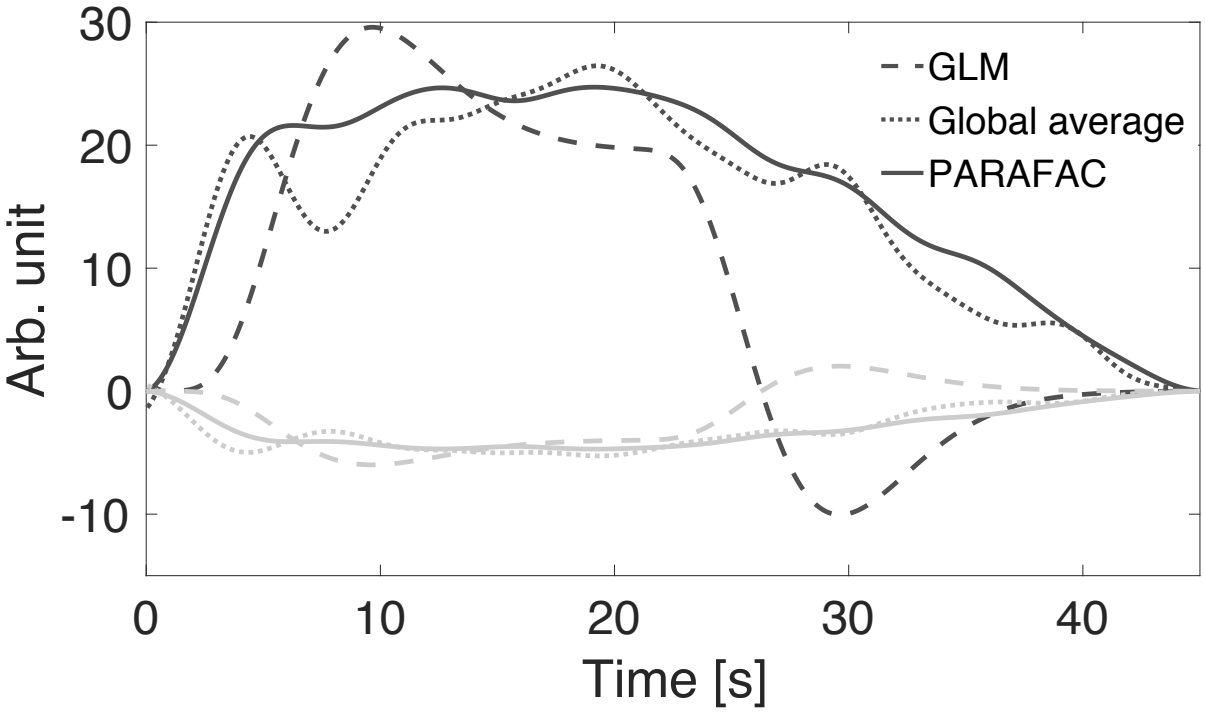

Figure 5. Description of the task-related brain activation pattern. Representative time course of hemodynamic response in the left Broca's area during the 30s verbal fluency task, as identified with the PARAFAC temporal component (solid line), modeled HRF as estimated by GLM (dashed line), and global averaged channels (dotted line). Black lines represent concentration changes in HbO, light grey lines are concentration changes in HbR.

6 Discussion

This study aimed to introduce and validate parallel factor analysis (PARAFAC), a multidimensional decomposition technique, for the analysis of fNIRS data. First, we investigated the efficacy of PARAFAC for the detection and correction of movement artifacts, as it would offer a very beneficial method in fNIRS. Second, we explored the usefulness of PARAFAC in identifying the dominant task-related activation in noisy experimental data. For both parts of our intended validation, results were compared to commonly used methods in fNIRS.

6.1 Artifact detection and correction

Several studies have shown promising results by using PARAFAC for artifact detection and correction, as well as to extract patterns of cerebral activation in EEG data (Martínez-Montes et al., 2004; Miwakeichi et al., 2004; Mørup et al., 2006). Our results are in line with these, expanding the application of PARAFAC for artifact correction and the extraction of cerebral activation patterns, thus extending the method's use in fNIRS.

Signal quality was evaluated using the SNR for segments in which artifacts were detected. All artifact correction techniques resulted in a significant improvement of the signal's quality, and thus a decrease of the noise in the artifact segments. ICA was applied, as reported in the literature, to the entire signal (H Zhang et al., 2010), while tPCA and PARAFAC were target-based, i.e. only decomposing the signal during specific segments where artifacts had been detected. In line with previous findings, our analyses reveal an advantage in applying target corrections (tPCA and PARAFAC) instead of whole-block (ICA) correction, resulting in a better signal quality (Behrendt et al., 2018; Yücel et al., 2014). Furthermore, comparisons between tPCA and PARAFAC suggest that the multidimensional approach of PARAFAC results in a slightly better correction. This means concentration changes in artifact segments after PARAFAC corrections achieved the smallest variance among the three methods. Nevertheless, it remains important to consider that the difference observed between tPCA and PARAFAC, though significant, has a small effect size, while the efficacy of PARAFAC is more robust as compared to ICA (large effect size). As proposed by Yücel et al. (2014), target artifact correction prevents change in the overall composition of the signal, and exclusively corrects the noisy time interval of the artifact. It allows the decomposition to clearly sort a component representing the artifact signature, without considering the characteristics of these channels during the intervals without artifacts. Target decomposition techniques are thus beneficial for a precise identification of the artifact's signature.

Signal quality was also evaluated using Pearson's correlation between the time course of both wavelengths, based on the assumption that different wavelengths (related to HbO and HbR concentrations) assessed at the same location are similarly affected by movement artifacts (Cui et al., 2010). Thus, the signal shows higher correlation between wavelengths when it reflects the same movement artifact, compared to a lower correlation for intervals where less or no artifact is present. Of the three different decomposition techniques, correction with PARAFAC led to the lowest correlation between HbO and HbR indices, as well as the correlation index that most resembles the non-artifactual baseline reference. Even though the resting-state signal has been reported to show slightly different hemodynamic changes, compared to the task-stimulation (Liu, 2013; Han Zhang et al., 2011), we consider it a suitable reference for a time interval without artifacts, because it should not be affected by articulation. Two-dimensional decomposition on the other hand, such as ICA and tPCA, analyzes both wavelengths as independent measures of the fNIRS signal, even though they are in fact highly related, since they are acquired at the same location (Cui et al., 2010)

Taken together, our results suggest that decomposition with PARAFAC allows an accurate detection and correction of artifacts. Decomposition with PARAFAC offers an approach whereby it is rather easy to make a selection of relevant components that differentiate between signatures related to artifacts or other relevant characteristics of the signal. Its efficacy resembles that obtained from tPCA, but its consideration of the intrinsically multidimensional structure of the fNIRS signal, as well as the absence of orthogonality or independence constraints, stand out as important advantages of PARAFAC. Even if fNIRS is considered to be less sensitive to movements, compared to other neuroimaging techniques such as fMRI, appropriate tools for artifact correction are essential, particularly for data acquired in populations where cooperation is limited, such as children and clinical populations (S Tak, Kempny, Friston, Leff, & Penny, 2015). PARAFAC thus appears to be a suitable alternative to the currently used approaches, and will be a valuable add-on for fNIRS studies and clinical examinations by minimizing the amount of non-usable data and improving data quality.

6.2 Characterizing fNIRS activation patterns

We applied a PARAFAC model with one single component, because by using the short-distance channel, we corrected our signal for systematic influences of physiology, and assumed that the remaining dominant signature represented the task-related cerebral activation. If there are empirical or theoretical reasons to expect more than one relevant component (e.g. resting state functional connectivity analysis, epileptic activity, physiological aspects, etc.), PARAFAC would also allow to for an increase in the number of components. In previous studies, the same semantic verbal fluency paradigm that we applied in our study reliably elicited typical cerebral activation within brain regions commonly associated with expressive language, namely the left Broca's area (Gaillard et al., 2003; Gallagher et al., 2016; Paquette et al., 2015). Therefore, we defined the ROI as the left Broca's area, as well as the homologous areas in the right hemisphere. We expected that roughly 5 seconds after task onset, the temporal and hemodynamic distributions would be reflected as an increase of HbO and a slight dip of HbR within the ROI (Glover, 1999).

The modeled time course indicates that, in contrast to GLM, both data-driven approaches, PARAFAC and global average, indicate an earlier onset of the hemodynamic response. A data-driven approach therefore provides more flexibility in paradigms or populations where cerebral activation may show alterations. Topographical representations of the task-related activation, on the other hand, does not clearly differ between GLM and global average. Our analysis of the mean relative weight of each channel for the PARAFAC component revealed significant task-related concentration changes in HbO and HbR within the ROI. This result was validated with the GLM and global average, which both showed a significant hemodynamic response within the ROI. PARAFAC, however, provides a slightly more distributed activation pattern, compared to both other approaches. Since the GLM imposes a modeled HRF with a specific time course, it may exclude channels with minor temporal deviations, an aspect that has been discussed critically on several previous studies (e.g. Monti, 2011; Scarpa et al., 2012). Global average intrinsically represents an approach to both minimizing variability and outlining the most constant information from the data, hence it is not surprising to obtain a more condensed spatial pattern. Both GLM and global average likely show the most dominant activation representing a more simplified pattern of cerebral activation. Topographical findings from PARAFAC reveal a brain activation that spreads into more cerebral regions known to be involved in expressive language processing (e.g. Hickok & Poeppel, 2000; Poeppel, Emmorey, Hickok, & Pylkkanen, 2012; Skeide & Friederici, 2016).

What is more, given that neither GLM nor global average treats HbO and HbR simultaneously, their results may only demonstrate strong concentration changes in either dimension, while ignoring the task-related dynamics of HbO and HbR. However, PARAFAC components are based on matrices that simultaneously consider time, space and hemodynamic dimensions, thus resulting in a component that considers the dynamics of both. Several studies have emphasized the importance of including both indices of concentration changes, in order to reliably interpret hemodynamic changes (Obrig et al., 2010; Quaresima et al., 2012; Wolf & Greisen, 2009). Applying PARAFAC for data analysis in fNIRS would allow a better exploitation of both HbO and HbR indices and their dynamics, hence leading to enriched results.

6.3 Integration and utility of PARAFAC

PARAFAC is a data-driven approach based on the linear relations of the three dimensions of the fNIRS signal (Bro, 1998; Martínez-Montes et al., 2004; Miwakeichi et al., 2004). PARAFAC has the advantage of allowing for the three-way arrays of data to be uniquely decomposed into a

sum of components, each of which is a trilinear combination of factors or signatures. One of the only statistical requirements of PARAFAC is that of a moderate linear independence across components, i.e. their time course, topography and wavelength characteristics. This is a less stringent requirement than previous models that underly space/time decompositions (PCA or ICA). Each component provides characteristics of a particular pattern identified within the correlation matrix. GLM and global average, on the other hand, treat each channel independently. These techniques provide a narrower spatial representation of the dominant activation compared to PARAFAC. In fact, PARAFAC analysis suggests a rather distributed activation pattern, while still revealing a dominant activation within our ROI. This strongly corresponds to the current understanding of cerebral processing, whereby large scale networks, and not isolated regions, are involved in language processing (e.g. Hickok & Poeppel, 2000; Poeppel et al., 2012; Skeide & Friederici, 2016). The use of PARAFAC to characterize hemodynamic patterns therefore appears to be more suitable for reflecting the cerebral processes occurring in distributed networks, rather than for the identification of a specific core region. Moreover, the topographic signature reflects the whole time course of the extracted activations, and can easily be subjected to diffusion optical tomography in order to locate the concentration changes in HbR and HbO in brain context (Tremblay et al., 2018).

Different from ICA, PARAFAC components can be ordered according to their importance in explaining the data's variance (e.g. Choi, Hwang, & Timmerman, 2018). This is why many studies using ICA apply data reduction or clustering techniques such as PCA prior to the execution of ICA (e.g. Makeig et al., 2002; H Zhang et al., 2010). When using PARAFAC, the description of data is based on more dimensions, and with less theoretical constraints (orthogonality, independence) which lead to the identification of fewer relevant components (Deburchgraeve et al., 2009; Martínez-Montes et al., 2004; Miwakeichi et al., 2004; Sidiropoulos & Bro, 2000). Compared to ICA, the selection of the relevant components is thus simplified. Importantly, when using PARAFAC, it is not recommended to ask for more than five components, as this increases the risk of overfitting the data with the decomposition model. Usually, three to five components sufficiently describe the signal's characteristics (Acar et al., 2007). Similarly to PCA, a typical choice made when using PARAFAC analysis, is that of ordering the extracted components according to their contribution to explaining the variance of the data. In this sense, it can be expected that the first PARAFAC component will always represent the highest activity, which, in the case of target artifact correction, will correspond to the artifact activity. This makes PARAFAC also a promising choice to explore the development of simple automatic methodologies for the detection and correction of such artifacts.

Some challenges of PARAFAC have already been discussed in previous studies (Martínez-Montes et al., 2004; Miwakeichi et al., 2004). First, PARAFAC assumes linear relations of the temporal characteristics between different channels. Despite being one of the most common and simple models, imposing linearity may not entirely reflect complex cerebral processes (Huppert, 2016). Some attempts have been made to introduce approaches that tolerate non-linear relations (e.g. Freiwald et al., 1999; Hu & Liang, 2014). However, to date, linear models remain the most popular approach for data analysis in neuroscience. Thus, it represents a general limit of the domain, rather than one specific to PARAFAC.

A second limitation regards the need for careful preprocessing of data before characterizing brain activity. When PARAFAC was introduced for the analysis of EEG data, the authors emphasized the importance of searching for constant factors, outliers, and degeneracy (Field & Graupe, 1991; Miwakeichi et al., 2004). Detailed information on how to deal with these aspects

can be found in previous literature (e.g. Miwakeichi et al., 2004). In the current study, the way PARAFAC has been implemented into the toolbox (LIONNIRS created by J. Tremblay, eng.) gave us a certain flexibility regarding the channels and time segments to be included. Thus, deviant channels were not considered.

An application of PARAFAC, not yet tested in fNIRS, is its use as a screening tool. For instance, Miwakeichi and colleagues (2004) applied PARAFAC to an EEG dataset in order to extract one component related to ocular movement artifacts, and subsequently used algorithms based on that component to screen a second dataset in order to identify and correct similar artifacts. Although this can be useful for correcting artifacts that have consistent topographical and wavelength profiles, in our study, movement artifacts were mostly related to articulation, often showing quite different signatures. A different paradigm may enable the testing of this application of PARAFAC in fNIRS.

Our findings also encourage the general application of PARAFAC for multidimensional decomposition in neuroimaging, where data can often be described on more than two dimensions. Beyond the obvious dimensions of a technique such as that of time × space × wavelength (fNIRS) or frequency (EEG), characteristics of the task paradigm or group variables could also be considered in the decomposition model (Mørup et al., 2006). For instance, if a "group" dimension was to be included, groups could be compared regarding their relative weight over the main cerebral activation component that would have been outlined from the PARAFAC model. There is thus potential for PARAFAC to become a tool for data analyses, because it takes advantage of the full richness of data sets in neuroscience.

6.4 Limits of the current study

The use of a language paradigm allowed for the induction of artifacts that were mainly related to articulation, which limits the generalization from our results. From video recordings, however, we were able to acknowledge that swallowing, jaw or tongue movements, eye blinks, and frowning also induced artifacts in our dataset. Further fNIRS studies using PARAFAC, and including different task paradigms and resting-state, would show its utility for a wider or different range of artifacts.

Another limitation related to the generalization of our results is the specific use of the simple least square technique to implement PARAFAC. Other methods have been proposed for estimating PARAFAC models, but some studies have shown that, given the uniqueness of the solution, they do not usually outperform the simple least square technique (Faber, Bro, & Hopke, 2003).

The validation of PARAFAC for artifact correction was conducted by comparing results with two other decomposition techniques. This could be considered one limit of the present study, because we did not consider other correction approaches for comparison. The objective of this study was not to conduct exhaustive and systematic comparisons in order to identify the best method for artifact correction, but rather to introduce PARAFAC as an alternative and adequate analysis method in fNIRS. Future studies could therefore advance the validation of PARAFAC and extend comparisons of its performance to other tools that do not necessarily use decomposition, such as spline interpolation or wavelet filtering. With relation to that, even if there were to be a slight advantage of PARAFAC over tPCA in artifact correction results, the small difference might not have a concrete impact on the applicability of those two methods. Qualitative differences between tPCA and PARAFAC regarding the type of artifacts and corrected signal should be further

assessed and described in subsequent studies, to better understand how their efficacy may vary according an artifact's characteristics.

7 Conclusion

PARAFAC allows for the simultaneous treatment of both wavelengths or HbO and HbR during fNIRS data analyses. Our findings validate previous findings in EEG data and promote multidimensional decomposition by use of PARAFAC as a promising new tool for the extraction of relevant signatures represented in the fNIRS signal. The validation of its use for the correction of movement artifacts, as well as to extract the pattern of a task-related cerebral activation, paves the way for its future use in the domain of fNIRS research.

8 Appendix

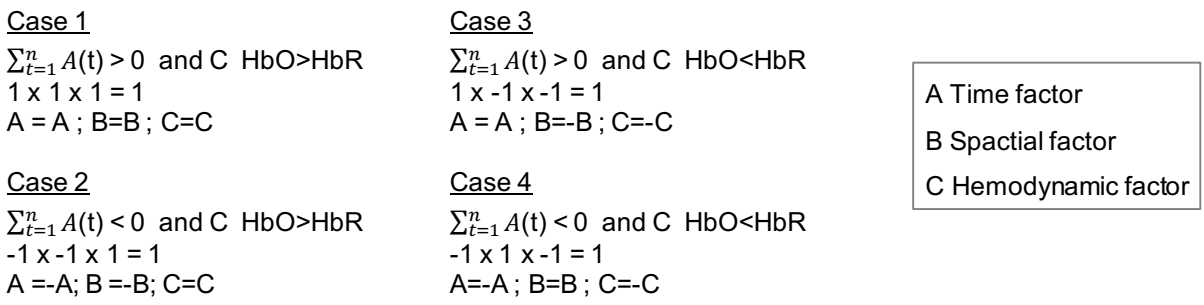

Figure 6. Positivity and negativity adjustment for PARAFAC component. Force HbO/HbR answer to be positive/negative in the sense that PARAFAC found 1x1x1 or 1x(-1)x(-1) without discrimination in the decomposition.

9 References

Aarabi, A., & Huppert, T. J. (2016). Characterization of the relative contributions from systemic physiological noise to whole-brain resting-state functional near-infrared spectroscopy data using single-channel independent component analysis. *Neurophotonics*, *3*(2), 025004. https://doi.org/10.1117/1.NPh.3.2.025004

Acar, E., Aykut-Bingol, C., Bingol, H., Bro, R., & Yener, B. (2007). Multiway analysis of epilepsy tensors. *Bioinformatics*, *23*(13), i10–i18. https://doi.org/10.1093/bioinformatics/btm210

Andersson, C. A., & Bro, R. (2000). The N-way Toolbox for MATLAB. *Chemometrics and Intelligent Laboratory Systems*, *52*(1), 1–4. https://doi.org/10.1016/S0169-7439(00)00071-X

Becker, H., Comon, P., Albera, L., Haardt, M., & Merlet, I. (2011). Multi-way space-time-wave-vector analysis for EEG source separation. *Signal Processing*, *92*, 1021–1031. https://doi.org/10.1016/j.sigpro.2011.10.014

Behrendt, H. F., Firk, C., Nelson, C. A., & Perdue, K. L. (2018). Motion correction for infant functional near-infrared spectroscopy with an application to live interaction data. *Neurophotonics*, *5*(01), 1. https://doi.org/10.1117/1.NPh.5.1.015004

Boas, D. a, Gaudette, T., Strangman, G., Cheng, X., Marota, J. J., & Mandeville, J. B. (2001). The accuracy of near infrared spectroscopy and imaging during focal changes in cerebral hemodynamics. *Neuroimage*, *13*(1), 76–90. https://doi.org/10.1006/nimg.2000.0674

Brigadoi, S., Ceccherini, L., Cutini, S., Scarpa, F., Scatturin, P., Selb, J., … Cooper, R. J. (2014). Motion artifacts in functional near-infrared spectroscopy: A comparison of motion correction techniques applied to real cognitive data. *NeuroImage*, *85*, 181–191. https://doi.org/10.1016/j.neuroimage.2013.04.082

Brigadoi, S., & Cooper, R. J. (2015). How short is short? Optimum source–detector distance for short-separation channels in functional near-infrared spectroscopy. *Neurophotonics*, *2*(2), 025005. https://doi.org/10.1117/1.NPh.2.2.025005

Bro, R. (1998). *Multi-way Analysis in the Food Industry Models, Algorithms, and Applications* (Royal Veterinary and Agricultural University). Retrieved from http://newton.foodsci.kvl.dk.

Bro, R., & De Jong, S. (1997). A fast non-negativity-constrained least squares algorithm. *Journal of Chemometrics*, *11*(5), 393–401. https://doi.org/10.1002/(SICI)1099-128X(199709/10)11:5<393::AID-CEM483>3.0.CO;2-L

Calhoun, V. (2018). Data-driven approaches for identifying links between brain structure and function in health and disease. *Dialogues in Clinical Neuroscience*, *20*(2), 87–99. Retrieved from http://www.ncbi.nlm.nih.gov/pubmed/30250386

Carroll, J. D., & Chang, J.-J. (1970). Analysis of individual differences in multidimensional scaling via an n-way generalization of “Eckart-Young” decomposition. *Psychometrika*, *35*(3), 283–319. https://doi.org/10.1007/BF02310791

Choi, J. Y., Hwang, H., & Timmerman, M. E. (2018). Functional Parallel Factor Analysis for Functions of One- and Two-dimensional Arguments. *Psychometrika*, *83*(1), 1–20. https://doi.org/10.1007/s11336-017-9558-9

Cohen, J. (1988). *Statistical Power Analysis for the Behavioral Sciences* (Second). New York, NY: Lawrence Erlbaum Associates, Inc.

Comon, P. (1994). Independent component analysis, A new concept? *Signal Processing*, *36*(3), 287–314. https://doi.org/10.1016/0165-1684(94)90029-9

Cooper, R. J., Selb, J., Gagnon, L., Phillip, D., Schytz, H. W., Iversen, H. K., … Boas, D. A. (2012). A systematic comparison of motion artifact correction techniques for functional near-infrared spectroscopy. *Frontiers in Neuroscience*, *6*(OCT), 1–10. https://doi.org/10.3389/fnins.2012.00147

Cui, X., Bray, S., & Reiss, A. L. (2010). Functional near infrared spectroscopy (NIRS) signal improvement based on negative correlation between oxygenated and deoxygenated hemoglobin dynamics. *NeuroImage*, *49*(4), 3039–3046. https://doi.org/10.1016/j.neuroimage.2009.11.050

Deburchgraeve, W., Cherian, P. J. J., De Vos, M., Swarte, R. M. M., Blok, J. H. H., Visser, G. H. H., … Van Huffel, S. (2009). Neonatal seizure localization using PARAFAC decomposition.

Clinical Neurophysiology, *120*(10), 1787–1796. Retrieved from https://www.sciencedirect.com/science/article/abs/pii/S1388245709004842

Faber, N. M., Bro, R., & Hopke, P. K. (2003, January 28). Recent developments in CANDECOMP/PARAFAC algorithms: A critical review. *Chemometrics and Intelligent Laboratory Systems*, Vol. 65, pp. 119–137. https://doi.org/10.1016/S0169-7439(02)00089-8

Field, A. S., & Graupe, D. (1991). Topographic component (Parallel Factor) analysis of multichannel evoked potentials: Practical issues in trilinear spatiotemporal decomposition. *Brain Topography*, *3*(4), 407–423. https://doi.org/10.1007/BF01129000

Freiwald, W. A., Valdes, P., Bosch, J., Biscay, R., Jimenez, J. C., Rodriguez, L. M., … Singer, W. (1999). Testing non-linearity and directedness of interactions between neural groups in the macaque inferotemporal cortex. *Journal of Neuroscience Methods*, *94*(1), 105–119. https://doi.org/10.1016/S0165-0270(99)00129-6

Friston, K. J., Ashburner, J. T., Kiebel, S. J., Nichols, T. E., & Penny, W. D. (2011). *Statistical Parametric Mapping: The Analysis of Functional Brain Images*. Retrieved from https://books.google.ca/books?hl=de&lr=&id=G_qdEsDlkp0C&oi=fnd&pg=PP1&dq=Friston,+K.,+Ashburner,+J.,+Kiebel,+S.,+Nichols,+T.,+Penny,+W.,+2011.+Statistical+Parametric+Mapping:+The+Analysis+of+Functional+Brain+Images:+The+Analysis+of+Functional+Brain+Images

Gaillard, W. D., Sachs, B. C., Whitnah, J. R., Ahmad, Z., Balsamo, L. M., Petrella, J. R., … Grandin, C. B. (2003). Developmental aspects of language processing: fMRI of verbal fluency in children and adults. *Human Brain Mapping*, *18*(3), 176–185. https://doi.org/10.1002/hbm.10091

Gallagher, A., Tremblay, J., & Vannasing, P. (2016). Language mapping in children using resting-state functional connectivity: comparison with a task-based approach. *Journal of Biomedical Optics*, *21*(12), 125006. https://doi.org/10.1117/1.JBO.21.12.125006

Glover, G. H. (1999). Deconvolution of Impulse Response in Event-Related BOLD fMRI1. *NeuroImage*, *9*(4), 416–429. https://doi.org/10.1006/nimg.1998.0419

Harshman, R. A. (1970). Foundations of the PARAFAC procedure: Models and conditions for an "explanatory" multimodal factor analysis (University Microfilms, Ann Arbor, Michigan; Vol. 16). Retrieved from http://www.psychology.uwo.ca/faculty/harshman/wpppfac0.pdf

Hickok, G., & Poeppel, D. (2000). Towards a functional neuroanatomy of speech perception. *Trends in Cognitive Sciences*, *4*(4), 131–138. https://doi.org/10.1016/S1364-6613(00)01463-7

Hu, M., & Liang, H. (2014). A copula approach to assessing Granger causality. *NeuroImage*, *100*, 125–134. https://doi.org/10.1016/j.neuroimage.2014.06.013

Huppert, T. J. (2016). Commentary on the statistical properties of noise and its implication on general linear models in functional near-infrared spectroscopy. *Neurophotonics*, *3*(1), 010401. https://doi.org/10.1117/1.NPh.3.1.010401

James, G., Witten, D., Hastie, T., & Tibshirani, R. (2013). Classification. In *An Introduction to Statistical Learning* (pp. 127–173). https://doi.org/10.1007/978-1-4614-7138-7_4

Jobsis, F. F. (1977). Noninvasive, infrared monitoring of cerebral and myocardial oxygen sufficiency and circulatory parameters. *Science (New York, N.Y.)*, *198*(4323), 1264–1267. https://doi.org/10.1126/SCIENCE.929199

Jung, A., Theis, F. J., Puntonet, C. G., & Lang, E. W. (2001). Fastgeo-a histogram based approach to linear geometric ICA. *Proceedings of ICA Vol. 1*, 349–354. Retrieved from http://citeseerx.ist.psu.edu/viewdoc/download?doi=10.1.1.16.924&rep=rep1&type=pdf

Jutten, C., & Herault, J. (1991). Blind separation of sources, part I: An adaptive algorithm based on neuromimetic architecture. *Signal Processing*, *24*(1), 1–10. https://doi.org/10.1016/0165-1684(91)90079-X

Kamran, M. A., Mannan, M. M. N., & Jeong, M. Y. (2016). Cortical Signal Analysis and Advances in Functional Near-Infrared Spectroscopy Signal: A Review. *Frontiers in Human Neuroscience*, *10*, 261. https://doi.org/10.3389/fnhum.2016.00261

Klem, G. H., Lüders, H. O., Jasper, H. H., & Elger, C. (1999). The ten-twenty electrode system of the International Federation. *Electroencephalogr Clin Neurophysiol*, *52*(3), 3–6. Retrieved from http://www.clinph-journal.com/pb/assets/raw/Health Advance/journals/clinph/Chapter1-1.pdf

Kocsis, L., Herman, P., & Eke, A. (2006). The modified Beer–Lambert law revisited. *Physics in Medicine and Biology*, *51*(5), N91–N98. https://doi.org/10.1088/0031-9155/51/5/N02

Liu, T. T. (2013). Neurovascular factors in resting-state functional MRI. *NeuroImage*, *80*, 339–348. https://doi.org/10.1016/J.NEUROIMAGE.2013.04.071

Lloyd-Fox, S., Blasi, A., & Elwell, C. E. (2010). Illuminating the developing brain: The past, present and future of functional near infrared spectroscopy. *Neuroscience and Behavioural Reviews*, *34*, 269–284. https://doi.org/10.1016/j.neubiorev.2009.07.008

Makeig, S., Westerfield, M., Jung, T. P., Enghoff, S., Townsend, J., Courchesne, E., & Sejnowski, T. J. (2002). Dynamic brain sources of visual evoked responses. *Science*, *295*(5555), 690–694. https://doi.org/10.1126/science.1066168

Martínez-Montes, E., Valdés-Sosa, P. A., Miwakeichi, F., Goldman, R. I., & Cohen, M. S. (2004). Concurrent EEG/fMRI analysis by multiway Partial Least Squares. *NeuroImage*, *22*(3), 1023–1034. https://doi.org/10.1016/j.neuroimage.2004.03.038

Minagawa-Kawai, Y., Van der Lely, H., Ramus, F., Sato, Y., Mazuka, R., & Dupoux, E. (2011). Optical brain imaging reveals general auditory and language-specific processing in early infant development. *Cerebral Cortex*, *21*(2), 254–261. https://doi.org/10.1093/cercor/bhq082

Miwakeichi, F., Martínez-Montes, E., Valdés-Sosa, P. A., Nishiyama, N., Mizuhara, H., & Yamaguchi, Y. (2004). Decomposing EEG data into space–time–frequency components using Parallel Factor Analysis. *NeuroImage*, *22*(3), 1035–1045. https://doi.org/10.1016/j.neuroimage.2004.03.039

Möcks, J. (1988). Decomposing event-related potentials: A new topographic components model. *Biological Psychology*, *26*(1–3), 199–215. https://doi.org/10.1016/0301-0511(88)90020-8

Monti, M. (2011). Statistical Analysis of fMRI Time-Series: A Critical Review of the GLM Approach. *Frontiers in Human Neuroscience*, *5*, 28. https://doi.org/10.3389/fnhum.2011.00028

Mørup, M., Hansen, L. K., Herrmann, C. S., Parnas, J., & Arnfred, S. M. (2006). Parallel Factor Analysis as an exploratory tool for wavelet transformed event-related EEG. *NeuroImage*, *29*(3), 938–947. https://doi.org/10.1016/j.neuroimage.2005.08.005

Obrig, H., Rossi, S., Telkemeyer, S., & Wartenburger, I. (2010). From acoustic segmentation to language processing: evidence from optical imaging. *Frontiers in Neuroenergetics*, *2*(13), 13. https://doi.org/10.3389/fnene.2010.00013

Paquette, N., Lassonde, M., Vannasing, P., Tremblay, J., Gonzalez-Frankenberger, B., Florea, O., … Gallagher, A. (2015). Developmental patterns of expressive language hemispheric lateralization in children, adolescents and adults using functional near-infrared spectroscopy. *Neuropsychologia*, *68*, 117–125. https://doi.org/10.1016/j.neuropsychologia.2015.01.007

Peng, K., Khoa Nguyen, D., Tayah, T., Vannasing, P., Tremblay, J., Sawan, M., … Pouliot, P. (2014). fNIRS-EEG study of focal interictal epileptiform discharges. *Epilepsy Research*, *108*, 491–505. https://doi.org/10.1016/j.eplepsyres.2013.12.011

Plank, M. (2013). Ocular correction ICA. *Brain Products Press Release*, *49*.

Poeppel, D., Emmorey, K., Hickok, G., & Pylkkanen, L. (2012). Towards a New Neurobiology of Language. *Journal of Neuroscience*, *32*(41), 14125–14131. https://doi.org/10.1523/JNEUROSCI.3244-12.2012

Quaresima, V., Bisconti, S., & Ferrari, M. (2012). A brief review on the use of functional near-infrared spectroscopy (fNIRS) for language imaging studies in human newborns and adults. *Brain and Language*, *121*(2), 79–89. https://doi.org/10.1016/j.bandl.2011.03.009

Scarpa, F., Brigadoi, S., Cutini, S., Scatturin, P., Zorzi, M., Dell'Acqua, R., & Sparacino, G. (2013). A reference-channel based methodology to improve estimation of event-related hemodynamic response from fNIRS measurements. *NeuroImage*, *72*, 106–119. https://doi.org/10.1016/j.neuroimage.2013.01.021

Scarpa, F., Fabris, C., Brigadoi, S., Cutini, S., Scatturin, P., Dell'Acqua, R., & Sparacino, G. (2012). *A GLM-Based Approach to Estimate Stimulus- Evoked Hemodynamic Response from fNIRS Measurements*. 736–739.

Schroeter, M. L., Bücheler, M. M., Müller, K., Uludağ, K., Obrig, H., Lohmann, G., … Von Cramon, D. Y. (2004). Towards a standard analysis for functional near-infrared imaging. *NeuroImage*, *21*(1), 283–290. https://doi.org/10.1016/j.neuroimage.2003.09.054

Schroeter, M. L., Kupka, T., Mildner, T., Uludağ, K., & von Cramon, D. Y. (2006). Investigating the post-stimulus undershoot of the BOLD signal—a simultaneous fMRI and fNIRS study. *NeuroImage*, *30*(2), 349–358. https://doi.org/10.1016/J.NEUROIMAGE.2005.09.048

Sidiropoulos, N. D., & Bro, R. (2000). On the uniqueness of multilinear decomposition of N-way arrays. *Journal of Chemometrics*, *14*(3), 229–239. https://doi.org/10.1002/1099-128X(200005/06)14:3<229::AID-CEM587>3.0.CO;2-N

Skeide, M. A., & Friederici, A. D. (2016). The ontogeny of the cortical language network. *Nature Reviews Neuroscience*, *17*(5), 323–332. https://doi.org/10.1038/nrn.2016.23

Sweeney, K. T., Ayaz, H., Ward, T. E., Izzetoglu, M., McLoone, S. F., & Onaral, B. (2012). A Methodology for Validating Artifact Removal Techniques for Physiological Signals. *IEEE Transactions on Information Technology in Biomedicine*, *16*(5), 918–926. https://doi.org/10.1109/TITB.2012.2207400

Tachtsidis, I., & Scholkmann, F. (2016). False positives and false negatives in functional near-infrared spectroscopy: issues, challenges, and the way forward. *Neurophotonics*, *3*(3), 031405. https://doi.org/10.1117/1.NPh.3.3.031405

Tak, S, Kempny, A. M., Friston, K. J., Leff, A. P., & Penny, W. D. (2015). Dynamic causal modelling for functional near-infrared spectroscopy. *NeuroImage*, *111*, 338–349. https://doi.org/10.1016/j.neuroimage.2015.02.035

Tak, Sungho, & Ye, J. C. (2014). Statistical analysis of fNIRS data: A comprehensive review. *NeuroImage*, *85*, 72–91. https://doi.org/10.1016/j.neuroimage.2013.06.016

Tremblay, J., Martinez-Montes, E., Vannasing, P., Nguyen, D. K., Sawan, M., Lepore, F., & Gallagher, A. (2018). Comparison of source localization techniques in diffuse optical tomography for fNIRS application using a realistic head model. *Biomedical Optics Express*, *9*(7), 448–454. https://doi.org/10.1364/BOE.9.002994

Tucker, L. R. (1966). Some mathematical notes on three-mode factor analysis. *Psychometrika*, *31*(3), 279–311. Retrieved from https://link.springer.com/content/pdf/10.1007%2FBF02289464.pdf

Villringer, A., & Dirnagl, U. (1995). Coupling of brain activity and cerebral blood flow: basis of functional neuroimaging. *Cerebrovascular and Brain Metabolism Reviews*, *7*(3), 240–276. Retrieved from http://www.ncbi.nlm.nih.gov/pubmed/8519605

Wolf, M., & Greisen, G. (2009). Advances in near-infrared spectroscopy to study the brain of the preterm and term neonate. *Clinics in Perinatology*, *36*(4), 807–834, vi. https://doi.org/10.1016/j.clp.2009.07.007

Yücel, M. A., Selb, J., Cooper, R. J., & Boas, D. A. (2014). Targeted principle component analysis: A new motion artifact correction approach for near-infrared spectroscopy. *Journal of Innovative Optical Health Sciences*, *7*(02), 1350066. https://doi.org/10.1142/S1793545813500661

Zhang, H, Zhang, Y.-J., Lu, C.-M., Ma, S.-Y., Zang, Y.-F., & Zhu, C.-Z. (2010). Functional connectivity as revealed by independent component analysis of resting-state fNIRS measurements. *NeuroImage*, *51*, 1150–1161. https://doi.org/10.1016/j.neuroimage.2010.02.080

Zhang, Han, Zhang, Y.-J., Duan, L., Ma, S.-Y., Lu, C.-M., & Zhu, C.-Z. (2011). Is resting-state functional connectivity revealed by functional near-infrared spectroscopy test-retest reliable? *Journal of Biomedical Optics*, *16*(6), 067008. https://doi.org/10.1117/1.3591020

Zhang, X., Noah, J. A., Dravida, S., & Hirsch, J. (2017). Signal processing of functional NIRS data acquired during overt speaking. *Neurophotonics*, *4*(04), 1. https://doi.org/10.1117/1.NPh.4.4.041409